

Assessing the Competitiveness of Matrix-Free Block Likelihood Estimation in Spatial Models

Alfredo Alegría*
Departamento de Matemática,
Universidad Técnica Federico Santa María,
Valparaiso, Chile

January 23, 2024

Abstract

In geostatistics, block likelihood offers a balance between statistical accuracy and computational efficiency when estimating covariance functions. This balance is reached by dividing the sample into blocks and computing a weighted sum of (sub) log-likelihoods corresponding to pairs of blocks. Practitioners often choose block sizes ranging from hundreds to a few thousand observations, inherently involving matrix-based implementations. An alternative, residing at the opposite end of this methodological spectrum, treats each observation as a block, resulting in the matrix-free pairwise likelihood method. We propose an additional alternative within this broad methodological landscape, systematically constructing blocks of size two and merging pairs of blocks through conditioning. Importantly, our method strategically avoids large-sized blocks, facilitating explicit calculations that ultimately do not rely on matrix computations. Studies with both simulated and real data validate the effectiveness of our approach, on one hand demonstrating its superiority over pairwise likelihood, and on the other, challenging the intuitive notion that employing matrix-based versions universally lead to better statistical performance.

Keywords: Cauchy covariance; Composite likelihood; Gaussian process; Godambe information; Large spatial datasets; Matérn covariance.

*The author gratefully acknowledges the support of Universidad Técnica Federico Santa María for grant *Proyectos Internos USM 2023 PI_LIR_23_11*.

1 Introduction

Gaussian processes constitute a fundamental mathematical framework for analyzing geostatistical data in diverse domains, including climatology, environmental sciences, geology, and ecology (Chiles and Delfiner, 2012; Cressie, 2015). Irrespective of the specific application context, accurately estimating the covariance function of the process is a pivotal step for meaningful analysis. This step enables a deeper understanding of the underlying dependence structure, allows for precise predictions at unsampled locations, and facilitates the quantification of uncertainties. These aspects are critical for ensuring reliable decision-making and effective risk assessment.

In the contemporary era, technological advancements enable the handling of large amounts of data, posing significant computational challenges to the feasibility of established inference and prediction methods. Specifically, when employing maximum likelihood estimation, a gold standard in statistics, it is customary to use Cholesky factorization as an intermediary process when calculating the determinant and inverse of the covariance matrix. However, the computational complexity of this procedure scales cubically with the sample size. In terms of memory requirements, the increase is quadratic. This challenge has prompted researchers to explore and design novel methodologies over the past decades, remaining a central focus in ongoing research. In recent competitions, various modern statistical methodologies, as documented in Heaton et al. (2019), Huang et al. (2021), and Hong et al. (2023), have demonstrated their relative strength in addressing this computational burden.

A variety of techniques utilize matrices with special characteristics to approximate the covariance matrix. These methods encompass the use of low-rank structures (Banerjee et al., 2008), hierarchical matrices (Litvinenko et al., 2020), sum of Kronecker products for gridded observations (Cao et al., 2021), and covariance tapering. The latter involves utilizing compactly supported covariance functions, resulting in sparse covariance matrices

suitable for specific numerical algorithms (Furrer et al., 2006; Kaufman et al., 2008; Shaby and Ruppert, 2012). Fast computation can also be achieved by approximating the inverse of the covariance matrix using the precision matrix of a Gaussian Markov process (Lindgren et al., 2011). Other approaches encompass employing Monte Carlo simulations to approximate score equations (Stein et al., 2013), exploring modified unbiased estimating equations that replace the covariance matrix with a sparse matrix (Sun and Stein, 2016), and utilizing techniques in the spectral domain, which allow computationally tractable approximations of the log-likelihood (Whittle, 1954; Fuentes, 2007).

The Vecchia approximation, introduced by Vecchia (1988), adopts a distinctive strategy by utilizing the product of conditional sub-likelihoods with small conditioning sets. This product serves as a substitute for the full likelihood. Essentially, it strategically focuses on conditional densities that involve neighboring observations, facilitating efficient computations while preserving key statistical information. For further insights and generalizations, see Stein et al. (2004) and Katzfuss and Guinness (2021).

Similarly, composite likelihood (CL) (Lindsay, 1988; Varin et al., 2011) constitutes a large family of inference techniques that employ the product of likelihoods for marginal or conditional events, following the "divide and conquer" principle. Due to their analytical and numerical simplicity, this manuscript specifically focuses on CL methods. CL is also distinguished by its considerable flexibility, demonstrated by its ability to effectively handle irregularly spaced data and its requirement for only the accurate specification of low-dimensional densities. Its efficacy in performing estimations has garnered extensive documentation in the spatial context, with references such as Curriero and Lele (1999), Caragea and Smith (2007), Bai et al. (2012), Bevilacqua et al. (2012), Eidsvik et al. (2014), Bevilacqua et al. (2016), and Ruli et al. (2016) offering comprehensive insights.

We concentrate on a variant of CL referred to as block likelihood. This involves dividing the sample into blocks, creating log-likelihoods for block pairs, and combining them addi-

tively with methodical weighting. The choice of a particular block size is determined by the user’s preferences for computational speed and the available computational resources. Certain alternatives use medium- or large-sized blocks to enhance the approximation of the full likelihood (Eidsvik et al., 2014), inherently involving matrix-based implementations. In this manuscript, when we mention ”large-sized” versions, we specifically allude to those that unavoidably depend on matrices. In contrast, the pairwise likelihood adopts a distinct approach by treating each individual observation as a block, representing the opposite end of the methodological spectrum. This avoids using matrices while maintaining a satisfactory level of statistical accuracy (Bevilacqua and Gaetan, 2015). Within this spectrum of variations, there are different possibilities, each aiming to achieve a balanced compromise between statistical and computational efficiencies.

In this study, we develop an additional matrix-free version of block likelihood, termed bi-conditional likelihood (bi-CL). This approach considers blocks of size two and systematically merges pairs of blocks through conditioning. This allows for the joint consideration of more information than conventional pairwise likelihood, achieving it without an increase in computational complexity, which is quadratic in the sample size. The conditional distribution utilized in our approach is bivariate, eliminating the need for matrix manipulation, as we provide an explicit formula for the objective function that does not ultimately rely on matrix operations. Moreover, we adopt the conventional and effective strategy of forming only a small number of pairs, not only to increase the speed of the method but also to enhance statistical efficiency.

While our approach is situated at an extreme segment in the extensive spectrum of block likelihood methods, our simulation studies, incorporating various correlation functions such as Exponential, Matérn, and Cauchy, reveal a notable advantage over pairwise likelihood. In some scenarios, our approach also demonstrates superior performance compared to versions employing large-sized blocks. Overall, we find that substantial increases in block sizes do

not consistently yield proportional statistical improvements. Moreover, we demonstrate the effectiveness of our methodology by applying it to sea surface temperature data. The dataset includes monthly measurements with a spatial resolution of 1° in both latitude and longitude, covering a substantial portion of the Earth. This dataset is provided by NOAA PSL in Boulder, Colorado, USA.

The article is organized as follows. Section 2 provides an overview of essential topics, including the geostatistical model, challenges related to maximum likelihood estimation, and a general perspective on composite likelihood methods. In Section 3, a detailed exploration of block-likelihood estimation is presented, followed by the introduction of the bi-CL method. Additionally, we provide guidance on blocking and weighting strategies, along with explanations of the code structure, available in a git repository. In Section 4, simulation studies are conducted, and Section 5 presents a real data example. Section 6 concludes the paper with a discussion.

2 Preliminaries

2.1 Geostatistical Model

Let $\{Z(\mathbf{s}) : \mathbf{s} \in \mathbb{R}^d\}$ be a real-valued Gaussian process, such that $\text{var}(Z(\mathbf{s})) < \infty$ for all $\mathbf{s} \in \mathbb{R}^d$. We assume that the process has zero mean, indicating prior detrending of the observed data. Moreover, in numerous real-world scenarios, correlations strengthen with spatial proximity and decline as distances increase, aligning with Tobler’s first law of geography and the principle known as isotropy (Chiles and Delfiner, 2012). To account for this behavior, we exclusively employ covariance functions based on distances.

Hence, for any pair of sites $\mathbf{s}, \mathbf{s}' \in \mathbb{R}^d$, the covariance function of the process can be expressed as

$$\text{cov}(Z(\mathbf{s}), Z(\mathbf{s}')) = \sigma^2 \rho(h; \phi),$$

where $h = \|\mathbf{s} - \mathbf{s}'\|$ represents the Euclidean distance between the locations. The function $\rho(\cdot; \boldsymbol{\phi})$ denotes a correlation function dependent on a vector of parameters $\boldsymbol{\phi} \in \mathbb{R}^q$. These parameters allow us to regulate important aspects, such as the shape and rate of decay of the correlation structure. Here, $\sigma^2 > 0$ is an additional parameter enabling control over the variance of the process.

Moreover, it is worth noting that numerous well-established parametric correlation functions $\rho(\cdot; \boldsymbol{\phi})$, specifically designed to guarantee the positive definiteness of the covariance matrix, including Matérn, Cauchy, spherical, wave, Wendland, and others, can be found in classical textbooks. For instance, interested readers may refer to Chapter 2 in [Chiles and Delfiner \(2012\)](#) for a comprehensive exploration of these functions. This diverse range of models has developed over the years to meet the specific challenges posed by a variety of real-world scenarios.

To enhance the model's versatility, it is common to incorporate a discontinuity in the covariance function at the origin, known as the nugget effect ([Chiles and Delfiner, 2012](#)). This extra mathematical element proves valuable in addressing the frequent occurrence of measurement errors that impact experimental data. The magnitude of this effect is regulated by a non-negative parameter, denoted as τ^2 . Consequently, the covariance function takes the form $\sigma^2\rho(h; \boldsymbol{\phi}) + \tau^2 1\{h = 0\}$, where $1\{\cdot\}$ represents the indicator function.

We assume that the process has been sampled at n locations $\mathbf{s}_1, \dots, \mathbf{s}_n$, which can either form a regular lattice, such as a network of soil sampling points systematically arranged, or be irregularly spaced, such as environmental monitoring stations in an urban area. We use the notation $Z_i = Z(\mathbf{s}_i)$ and consider the vector of data $\mathbf{Z} = (Z_1, \dots, Z_n)^\top$, where $^\top$ denotes the transpose operator. Then, $\mathbf{Z} \sim \mathcal{N}_n(\mathbf{0}, \sigma^2 \mathbf{R}(\boldsymbol{\phi}) + \tau^2 \mathbf{I}_n)$, where \mathbf{I}_n is the $n \times n$ identity matrix, and the (i, j) -th entry of $\mathbf{R}(\boldsymbol{\phi})$ is given by $\rho(\|\mathbf{s}_i - \mathbf{s}_j\|; \boldsymbol{\phi})$ for each $i, j = 1, \dots, n$.

The estimation of the parameters can be performed by maximizing the log-likelihood

function, which, up to a positive constant, is given by

$$\ell(\tau^2, \sigma^2, \boldsymbol{\phi}) = -\frac{1}{2} \left(\log |\sigma^2 \mathbf{R}(\boldsymbol{\phi}) + \tau^2 \mathbf{I}_n| + \mathbf{Z}^\top [\sigma^2 \mathbf{R}(\boldsymbol{\phi}) + \tau^2 \mathbf{I}_n]^{-1} \mathbf{Z} \right), \quad (1)$$

where $|\cdot|$ denotes the determinant. However, evaluating the determinant and the inverse in (1) poses a substantial challenge for scientists dealing with large sample sizes and irregularly sited locations, involving $O(n^{2.81})$ steps (see, e.g., [Aho and Hopcroft, 1974](#)). Traditional algorithms such as Cholesky decomposition have a complexity of $O(n^3)$. This challenge has prompted scientists to explore new statistical methodologies for conducting inferences.

2.2 Composite Likelihood

The composite likelihood (CL) estimation framework (refer, for example, to [Lindsay, 1988](#); [Varin et al., 2011](#)) considers the following paradigm: provided a set of marginal or conditional data segments A_k , $k = 1, \dots, K$, along with their corresponding log-likelihood functions $\ell_k(\boldsymbol{\theta})$, the CL estimates are obtained by maximizing the objective function

$$\text{CL}(\boldsymbol{\theta}) = \sum_{k=1}^K \omega_k \ell_k(\boldsymbol{\theta}). \quad (2)$$

Here, for the sake of simplifying the exposition, we have denoted the vector of parameters as $\boldsymbol{\theta} = (\tau^2, \sigma^2, \boldsymbol{\phi}^\top)^\top$, while $\omega_1, \dots, \omega_K$ represent appropriate weights designed to enhance the statistical and computational efficiency of the method. This approach is a misspecified likelihood, where the misspecification originates from assuming independence among segments. Methods in this class offer a balance between statistical and computational efficiency, as the segments of data yield sub-likelihoods that are more computationally cost-effective.

Given that (2) is expressed as the sum of (sub) log-likelihoods, it serves as an unbiased estimation equation. Assuming adequate regularity conditions ([Varin, 2008](#)), the composite likelihood estimator is consistent and asymptotically Gaussian under increasing domain asymptotics (i.e., when the spatial domain expands with the increasing number of locations). In such a context, we must consider the Godambe information matrix, defined

as

$$G(\boldsymbol{\theta}) = H(\boldsymbol{\theta})J(\boldsymbol{\theta})^{-1}H(\boldsymbol{\theta}),$$

where $H(\boldsymbol{\theta}) = E(-\nabla^2 \text{CL}(\boldsymbol{\theta}))$ and $J(\boldsymbol{\theta}) = E(\nabla \text{CL}(\boldsymbol{\theta})\nabla \text{CL}(\boldsymbol{\theta})^\top)$, with ∇^2 and ∇ representing the Hessian and gradient, respectively. The asymptotic variance of the composite likelihood estimator is given by the inverse of the Godambe information matrix.

While the primary focus of exploring CL methods in this work is achieving computational efficiency in Gaussian processes, in alternative contexts, the motivation comes from the inherent analytical complexities of expressing likelihood functions in a closed form. This analytical challenge becomes especially pronounced when dealing with some classes of non-Gaussian processes, where obtaining finite-dimensional distributions becomes intricate. Notably, both analytical and computational challenges may appear simultaneously in certain geostatistical models. To further explore the application of CL methods to spatial data, especially when dealing with distinctive features that deviate from the Gaussian assumption, such as skewness, binary structure, or the study of extreme spatial events, we recommend consulting the works of [Heagerty and Lele \(1998\)](#), [Sang and Genton \(2014\)](#), [Castruccio et al. \(2016\)](#), and [Alegría et al. \(2017\)](#).

3 Block Likelihood Estimation

3.1 The Spectrum of Block Likelihood

We restrict our attention to a specific category of CL methods, referred to as block likelihood. This approach, proposed by [Eidsvik et al. \(2014\)](#), involves dividing the data into m pieces. A partition $\Delta = \{b_1, \dots, b_m\}$ of the set $\{1, \dots, n\}$ is considered, where the i -th block of data is defined as $\mathbf{Z}_{b_i} = (Z_j : j \in b_i)$, for $i = 1, \dots, m$. The cardinality of b_i is denoted by m_i . [Eidsvik et al. \(2014\)](#) considered pairs of blocks $\mathbf{Z}_{b_i, b_j} = (\mathbf{Z}_{b_i}^\top, \mathbf{Z}_{b_j}^\top)^\top$, each

with a corresponding log-likelihood

$$\ell_{b_i, b_j}(\tau^2, \sigma^2, \boldsymbol{\phi}) = -\frac{1}{2} \left(\log |\sigma^2 \mathbf{R}_{b_i, b_j}(\boldsymbol{\phi}) + \tau^2 \mathbf{I}_{m_i + m_j}| + \mathbf{Z}_{b_i, b_j}^\top [\sigma^2 \mathbf{R}_{b_i, b_j}(\boldsymbol{\phi}) + \tau^2 \mathbf{I}_{m_i + m_j}]^{-1} \mathbf{Z}_{b_i, b_j} \right),$$

where $\mathbf{R}_{b_i, b_j}(\boldsymbol{\phi})$ denotes the sub-matrix of $\mathbf{R}(\boldsymbol{\phi})$ associated to \mathbf{Z}_{b_i, b_j} . The objective function of the block likelihood method is given by

$$\text{BCL}_m(\tau^2, \sigma^2, \boldsymbol{\phi}) = \sum_{i=1}^{m-1} \sum_{j=i+1}^m \omega_{ij} \ell_{b_i, b_j}(\tau^2, \sigma^2, \boldsymbol{\phi}).$$

The subscript m highlights the method's dependence on the number of considered blocks. Additionally, there is a significant dependence on the chosen configuration for the blocks Δ ; however, we omit this to prevent the notation from becoming too intricate.

When $m = 1$ or $m = 2$, the full likelihood is recovered. Conversely, increasing the number of blocks renders the problem more computationally tractable, as it necessitates computing determinants and inverses of smaller matrices. In the limit, if we consider n blocks of the form $b_i = \{i\}$, i.e., treating each individual observation as a block, we obtain the pairwise composite likelihood (referred to by the acronym PCL) method, whose objective function simplifies to

$$\text{PCL}(\sigma^2, \boldsymbol{\phi}) = -\frac{1}{2} \sum_{i=1}^{n-1} \sum_{j=i+1}^n \omega_{ij} \left(\log \left((\sigma^2 + \tau^2)^2 - (\sigma^2 \rho_{ij})^2 \right) + \frac{(\sigma^2 + \tau^2) (Z_i^2 + Z_j^2) - 2\sigma^2 \rho_{ij} Z_i Z_j}{(\sigma^2 + \tau^2)^2 - (\sigma^2 \rho_{ij})^2} \right), \quad (3)$$

where the notation $\rho_{ij} = \rho(\|\mathbf{s}_i - \mathbf{s}_j\|; \boldsymbol{\phi})$ seeks to abbreviate the preceding expression. A notable feature of PCL is that it obviates the need to manipulate matrices, given the explicit expression (3). Although other matrix-free CL versions based on conditioning or differences of pairs exist (Curriero and Lele, 1999; Bevilacqua and Gaetan, 2015), we focus on (3), as other versions generally exhibit equal or inferior performance, as documented in Bevilacqua and Gaetan (2015).

Figure 1 illustrates the spectrum of block likelihood inference with respect to the employed block sizes. It positions the two extreme cases, full likelihood, and PCL, at the ends

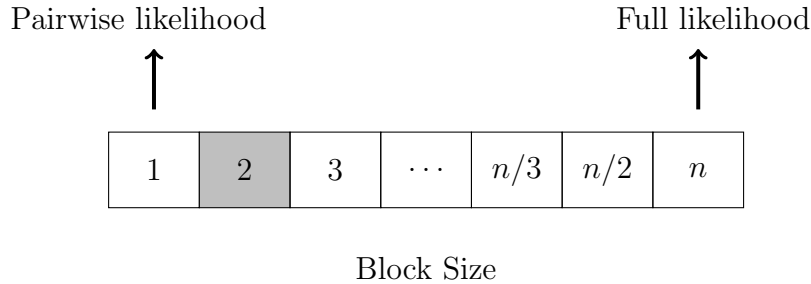


Figure 1: Spectrum of block likelihood estimation, categorized by the employed block sizes. The shaded box illustrates the utilization of blocks of size two, which is the basis for the matrix-free bi-conditional likelihood method introduced in Section 3.2.

of this spectrum. It is important to note that this example is idealized; in real applications, the sizes of utilized blocks may vary based on the distribution of sites and the specific value of n . This idealization serves as a visual aid in understanding the methodological landscape.

In the PCL method, as distant pairs of data tend to exhibit weaker correlations, their contribution to the estimation process is relatively limited. Hence, it is common to employ a 0/1 structure for ω_{ij} . More precisely, the following weights are considered

$$\omega_{ij} = \begin{cases} 1 & \text{if } \|\mathbf{s}_i - \mathbf{s}_j\| < d_s \\ 0 & \text{otherwise} \end{cases},$$

where $d_s > 0$ is a predefined threshold. This not only improves computational performance but also has the potential to enhance statistical efficiency. This concept has been extensively discussed in the literature and was recently explored in depth by [Caamaño-Carrillo et al. \(2024\)](#), where pairs are formed solely based on the locations of nearest neighbors.

In the context of block likelihood, with large-sized blocks, a similar weighting strategy can be applied, interpreting the distance between blocks in relation to their centers of mass or employing concepts of neighboring blocks (refer to [Eidsvik et al., 2014](#)).

3.2 The Bi-Conditional Likelihood

In this section, we develop a methodology within the context of the block likelihood approaches discussed earlier. We start by introducing notation to facilitate the formulation of the objective function. Let $\Omega = \{\mathbf{s}_1, \dots, \mathbf{s}_n\}$ denote the set of locations. Assume n is even (in the case of odd n , one location must be excluded initially). We partition the set Ω into $\Omega = \bigcup_{i=1}^{n/2} \Omega_i$, where each subset Ω_i comprises two sites, \mathbf{s}_i^a and \mathbf{s}_i^b , for all $i = 1, \dots, n/2$. We define $Z_i^a = Z(\mathbf{s}_i^a)$, $Z_i^b = Z(\mathbf{s}_i^b)$, and $\mathbf{Z}_i = (Z_i^a, Z_i^b)^\top$. We also consider $\rho_{ij}^{ab} = \rho(\|\mathbf{s}_i^a - \mathbf{s}_j^b\|; \boldsymbol{\phi})$, $\rho_{ij}^{aa} = \rho(\|\mathbf{s}_i^a - \mathbf{s}_j^a\|; \boldsymbol{\phi})$, and $\rho_{ij}^{bb} = \rho(\|\mathbf{s}_i^b - \mathbf{s}_j^b\|; \boldsymbol{\phi})$, for $i, j = 1, \dots, n/2$.

We will be working with the random vectors $\mathbf{U}_{ij} = \mathbf{Z}_i | \mathbf{Z}_j$, for $i \neq j$. This is the reason we refer to this method as bi-conditional likelihood (bi-CL). To derive explicit expressions for the distribution of \mathbf{U}_{ij} , it is worth noting that $(\mathbf{Z}_i^\top, \mathbf{Z}_j^\top)^\top$ follows a quadri-variate Gaussian distribution, with zero mean, and covariance matrix

$$\begin{bmatrix} \boldsymbol{\Sigma}_{11} & \boldsymbol{\Sigma}_{12} \\ \boldsymbol{\Sigma}_{21} & \boldsymbol{\Sigma}_{22} \end{bmatrix} = \left[\begin{array}{cc|cc} \sigma^2 + \tau^2 & \sigma^2 \rho_{ii}^{ab} & \sigma^2 \rho_{ij}^{aa} & \sigma^2 \rho_{ij}^{ab} \\ & \sigma^2 + \tau^2 & \sigma^2 \rho_{ij}^{ba} & \sigma^2 \rho_{ij}^{bb} \\ \hline & & \sigma^2 + \tau^2 & \sigma^2 \rho_{jj}^{ab} \\ & & & \sigma^2 + \tau^2 \end{array} \right].$$

We have excluded the values below the main diagonal, considering the matrix's symmetry. Consequently, $\mathbf{Z}_i | \mathbf{Z}_j = \mathbf{z}_j$ follows a bivariate Gaussian distribution with a mean of $\boldsymbol{\Sigma}_{12} \boldsymbol{\Sigma}_{22}^{-1} \mathbf{z}_j$ and a covariance matrix of $\boldsymbol{\Sigma}_{11} - \boldsymbol{\Sigma}_{12} \boldsymbol{\Sigma}_{22}^{-1} \boldsymbol{\Sigma}_{21}$, facilitating the derivation of its log-likelihood function $\ell_{ij}^{(\text{bi})}(\tau^2, \sigma^2, \boldsymbol{\phi})$.

Defining the elements of $\boldsymbol{\Sigma}_{12} \boldsymbol{\Sigma}_{22}^{-1}$ as auxiliary quantities not only allows us to readily derive a closed-form expression for the objective function but also contributes to the simplification of the coding process. Indeed, consider the quantities

$$\bullet \psi_{11} = \sigma^2 \left[\frac{(\sigma^2 + \tau^2) \rho_{ij}^{aa} - \sigma^2 \rho_{ij}^{ab} \rho_{jj}^{ab}}{(\sigma^2 + \tau^2)^2 - (\sigma^2 \rho_{jj}^{ab})^2} \right] \quad \bullet \psi_{21} = \sigma^2 \left[\frac{(\sigma^2 + \tau^2) \rho_{ij}^{ba} - \sigma^2 \rho_{ij}^{bb} \rho_{jj}^{ab}}{(\sigma^2 + \tau^2)^2 - (\sigma^2 \rho_{jj}^{ab})^2} \right]$$

$$\bullet \psi_{12} = \sigma^2 \left[\frac{(\sigma^2 + \tau^2)\rho_{ij}^{ab} - \sigma^2\rho_{ij}^{aa}\rho_{jj}^{ab}}{(\sigma^2 + \tau^2)^2 - (\sigma^2\rho_{jj}^{ab})^2} \right] \quad \bullet \psi_{22} = \sigma^2 \left[\frac{(\sigma^2 + \tau^2)\rho_{ij}^{bb} - \sigma^2\rho_{ij}^{ba}\rho_{jj}^{ab}}{(\sigma^2 + \tau^2)^2 - (\sigma^2\rho_{jj}^{ab})^2} \right]$$

Thus, performing a straightforward calculation, we obtain

$$\ell_{ij}^{(\text{bi})}(\tau^2, \sigma^2, \phi) = -\frac{1}{2} \left[\log(\eta) + \frac{\xi_{22}(Z_i^a - \mu_1)^2 + \xi_{11}(Z_i^b - \mu_2)^2 - 2\xi_{12}(Z_i^a - \mu_1)(Z_i^b - \mu_2)}{\eta} \right],$$

where

$$\begin{aligned} \bullet \xi_{11} &= \tau^2 + \sigma^2(1 - \psi_{11}\rho_{ij}^{aa} - \psi_{12}\rho_{ij}^{ab}) & \bullet \mu_1 &= \psi_{11}Z_j^a + \psi_{12}Z_j^b \\ \bullet \xi_{12} &= \sigma^2(\rho_{ii}^{ab} - \psi_{11}\rho_{ij}^{ba} - \psi_{12}\rho_{ij}^{bb}) & \bullet \mu_2 &= \psi_{21}Z_j^a + \psi_{22}Z_j^b \\ \bullet \xi_{22} &= \tau^2 + \sigma^2(1 - \psi_{21}\rho_{ij}^{ba} - \psi_{22}\rho_{ij}^{bb}) & \bullet \eta &= \xi_{11}\xi_{22} - \xi_{12}^2 \end{aligned}$$

Finally, the objective function for the bi-CL method is constructed following the conventional additive weighted methodology:

$$\text{bi-CL}(\tau^2, \sigma^2, \phi) = \sum_{i=1}^{n/2} \sum_{j \neq i}^{n/2} \omega_{ij} \ell_{ij}^{(\text{bi})}(\tau^2, \sigma^2, \phi).$$

Remark 3.1 *Let us highlight some remarks on this methodology.*

1. *While bi-CL can be categorized as a form of block likelihood, our approach distinguishes itself by employing conditioning to merge the blocks. This strategy prevents a substantial increase in dimensionality and facilitates explicit calculations that ultimately do not rely on matrix computations.*
2. *By interlacing bi-dimensional blocks, we anticipate achieving a potentially more robust integration of statistical information compared to the PCL method. This improvement is achieved while essentially retaining the same computational cost, with the order of computation for forming all possible pairs of blocks being $O((n/2)^2)$. Consequently, we expect our approach presenting a more competitive alternative within the segment of matrix-free block likelihoods.*

3. It is straightforward to see that $\ell_{ij}^{(bi)}$ can be expressed as the difference between the log-likelihood of the vector $(Z_i^a, Z_i^b, Z_j^a, Z_j^b)^\top$ and the log-likelihood of the pair $(Z_j^a, Z_j^b)^\top$. This implies that the objective function of bi-CL is an additive combination of two functions originating from the method developed by [Eidsvik et al. \(2014\)](#).
4. By building our proposal upon the architecture of an established method, the estimates inherit the favorable properties of consistency and asymptotic normality, under adequate regularity conditions in an increasing domain regime ([Varin, 2008](#)). Additionally, from a computational perspective, the method inherits compatibility with parallel computing and the possibility to load portions of data into memory separately.

3.3 Guidelines for Partitioning and Weighting

The bi-CL method significantly relies on the design of blocks. In this study, we adopt a strategy that entails grouping spatial sites in proximity to each other, with the aim of improving the methods' performance. This strategy has been widely utilized and has proven beneficial in enhancing the performance of CL methods ([Bai et al., 2012](#); [Bevilacqua and Gaetan, 2015](#); [Caamaño-Carrillo et al., 2024](#)).

Specifically, we randomly sample $n/2$ points uniformly distributed in the region of interest and gradually form blocks by grouping the two nearest neighbor locations to a given simulated point. The design may vary across experiments, depending on the fixed order of simulated points that determines the grouping sequence. Nevertheless, despite this variability, the architecture consistently approximates the desired proximity features.

In [Figure 2](#), we illustrate this process for 12 sites (see the first panel). Following this scheme, we can create six blocks of size 2, each labeled with the corresponding number to simplify the illustration (as shown in the second panel). Repeating this procedure once more produces another configuration, yet in alignment with the same principles (third panel). When forming pairs of blocks, points that interact in the first configuration may not do so

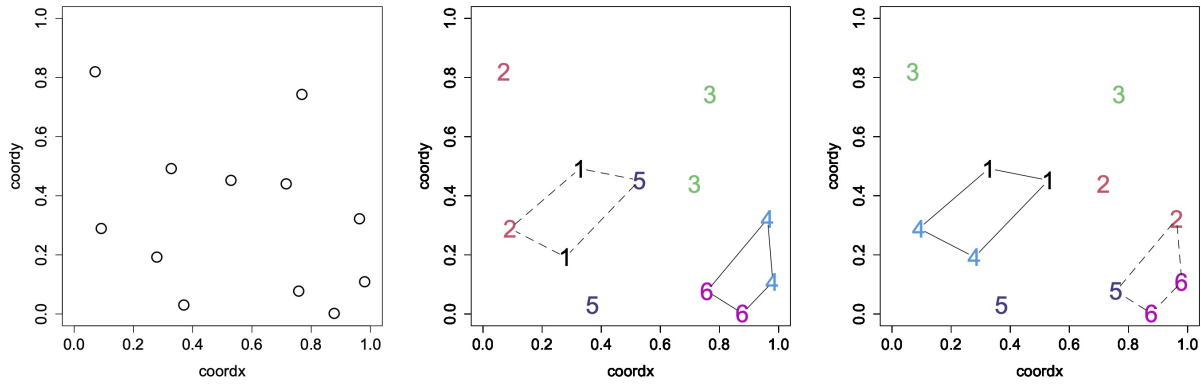


Figure 2: From left to right: 12 spatial sites and two possible configurations with 6 bi-dimensional blocks. Pairs of blocks that are part of the objective function are symbolized by the solid line connecting them, while the dashed line represents a list of sites that do not interact simultaneously for that configuration.

in the second (and vice versa). For example, in the second panel of Figure 2, the four points connected by the dashed line involve three different blocks (1, 2, and 5). Consequently, they will not interact simultaneously in the objective function, as the approach relies only on pairs of blocks. However, in the configuration of the third panel, these four sites have been labeled differently, such that they exactly coincide to be the members of blocks 1 and 4. Therefore, they will be part of the objective function simultaneously, as indicated by a solid line connecting them. In the bottom right of the figure, a similar example is illustrated, highlighting points that interact in the first configuration (solid line in the second panel) but not in the second (dashed line in the third panel).

Therefore, we recommend creating multiple configurations and aggregating their respective objective functions additively. This approach forms a more robust overall objective function that involves more interaction among closely observed data points.

For the weights, we will consider the following strategy, which is similar to the weights

previously discussed for PCL:

$$\omega_{ij} = \begin{cases} 1 & \text{if } \|\mathbf{s}_i^a - \mathbf{s}_j^a\| < d_s \\ 0 & \text{otherwise} \end{cases},$$

for some positive constant d_s . In essence, we compare the first element of each block, and if their distance is below a given threshold, this pair enters the objective function.

Note that the bi-CL method provides additional degrees of freedom, allowing for the creation of even more intricate weights. For instance, one could define weights based on factors such as maximum, minimum, or average element-wise distance between blocks. Nevertheless, we adhere to the aforementioned choice for its simplicity. The subsequent sections demonstrate that this preference yields favorable results. Given the proposed strategy for grouping sites, we anticipate that any of these alternatives are expected to result in similar performances of the method.

3.4 Implementation Details

In the GitHub repository https://github.com/alfredoalegria/bi_CL, we provide an R script exemplifying the method and the implementation of the described guidelines for partitioning. Supplementary auxiliary files are also included for modular code organization, incorporating functionalities from both R and C languages to enhance execution efficiency.

In particular, the objective function is computed using the function found in the file `bi_cl.c`, taking advantage of the inherent speed benefits of the C programming language. Additionally, we designed the `partition` function, utilizing specific features of R to facilitate the sample partitioning process.

As previously outlined, the method’s construction relies on initially labeling half of the sites with the symbol "a" and the remaining half with the symbol "b", followed by the corresponding partitioning of the data vector. We focus on processes on the plane. Thus, the primary inputs for the `bi_cl` function include:

- a list of x and y coordinates for points labeled with "a" (`cx_a` and `cy_a`);
- a list of x and y coordinates for points labeled with "b" (`cx_b` and `cy_b`);
- corresponding partitioning of the data vector (`z_a` and `z_b`):
- additional key variables are the number of blocks (`m`), the threshold for weights (`ds`), the chosen correlation model (`choice`), and parameter values (`s2`, `range`, `tau2`).

4 Simulation Studies

In this section, we assess the statistical and computational efficiency of diverse block likelihood estimation methods across different scenarios. This encompasses an examination of matrix-free and large-sized blocking structures in comparison to the full likelihood. From now on, we will exclusively use the acronym BCL to refer to the block likelihood with large blocks, distinguishing it from PCL and bi-CL, each having its own designated acronyms.

4.1 Simulation Setup

We will focus on the following families of correlation functions:

- Exponential model: $\rho(h; \phi) = \exp\left(-\frac{3h}{\phi}\right)$.
- Matérn (1.5) model: $\rho(h; \phi) = \exp\left(-\frac{4.7619h}{\phi}\right) \left(1 + \frac{4.7619h}{\phi}\right)$.
- Cauchy model: $\rho(h; \phi) = \left(1 + \left(\frac{4.3588h}{\phi}\right)^2\right)^{-1}$.

All models have been parameterized in terms of a range parameter ϕ ; that is, the correlation is smaller than 0.05 when $h > \phi$. The first two models are special cases of the Matérn family of correlation functions, with shape parameters of 0.5 and 1.5, respectively. This parameter governs the degree of smoothness of the correlation function at the origin, playing a crucial role in characterizing the level of differentiability (in a mean square sense) of the

process (see, e.g., [Stein, 2012](#)). Hence, the realizations from the Matérn (1.5) model exhibit greater smoothness compared to those generated by the exponential model. On the other hand, the Cauchy model is characterized by polynomial decay, in contrast to Matérn-type models, which exhibit exponential decay. This polynomial decay allows for a more persistent correlation between observations even when separated by large distances.

We consider the spatial domain $[0, 1]^2$ and the following values for the range: 0.10, 0.15, and 0.20. In summary, these scenarios encompass different degrees of smoothness, representing the most typical ones used in practice. They also feature distinct correlation decay structures, such as exponential and polynomial, along with three correlation ranges, representing processes with diverse levels of association. In all our experiments, we set $\sigma^2 = 1$ and $\tau^2 = 0.1$, resulting in the parameter vector $\boldsymbol{\theta} = (\tau^2, \sigma^2, \phi)^\top$.

We will be working with a set of $n = 500$ irregularly distributed sites. This moderate sample size allows for comparisons with the full likelihood. The generation of these sites adheres to the method outlined in [Bevilacqua and Gaetan \(2015\)](#): initially creating a regular grid with increments of 0.03 over $[0, 1]^2$, we then perturb each location by adding a uniform random value from $[-0.01, 0.01]$ to each coordinate. Finally, we randomly select 500 points without replacement.

To maximize the objective functions, we employed a Nelder–Mead algorithm, allowing a maximum of 10^4 iterations and a convergence tolerance of 10^{-16} between successive iterates. Given that we estimate three parameters, these specifications proved sufficient to attain accurate results for all scenarios; in fact, the number of iterations was only a few hundreds for all the experiments, and the method consistently converged to a solution without encountering any issues of degeneracy.

4.2 Bi-CL vs. PCL

We benchmark bi-CL against its closest competitor in the block likelihood spectrum, the PCL method, both being matrix-free approaches. Both methods are implemented with 0/1 weights, where the threshold d_s takes values of 0.05, 0.10 and 0.15. We added five configurations to implement the bi-CL method. We assess their effectiveness across the aforementioned scenarios and models, in comparison to the full likelihood (ML). The assessment involves computing relative root mean square errors for each parameter through Monte Carlo simulations, with 1000 independent repetitions. We also assess the overall effectiveness using a global measure:

$$\left(\frac{|\mathbf{G}_{\text{ML}}|^{1/2}}{|\mathbf{G}_{\text{CL}}|^{1/2}} \right)^{1/3},$$

where $\mathbf{G}_{\text{ML}} = 1000^{-1} \sum_{i=1}^{1000} (\hat{\boldsymbol{\theta}}_i^{\text{ML}} - \boldsymbol{\theta})(\hat{\boldsymbol{\theta}}_i^{\text{ML}} - \boldsymbol{\theta})^\top$. The matrices associated with the PCL and bi-CL methods, denoted here as \mathbf{G}_{CL} , are defined in a similar fashion. The metric involves the cubic root, as there are three parameters.

The results are displayed in Tables 1, 2 and 3, for the exponential, Matérn (1.5) and Cauchy models, respectively. In all scenarios, the bi-CL method consistently outperforms PCL. In the case of the exponential model, both methods demonstrate good performance. For example, when the range is 0.1 and the methods are implemented with $d_s = 0.1$, PCL demonstrates a global performance of 91.03%, while bi-CL achieves 93.87%. Observe that PCL exhibits poor performance when $d_s = 0.05$ (i.e., when a drastically sparse weighting scheme is adopted), while bi-CL remains more stable. The differences between both methods become more pronounced for the Matérn (1.5) and Cauchy models. For instance, when the range is 0.1, the efficiency of bi-CL is 90.85% in the Matérn (1.5) class, while the efficiency of PCL decreases to 83.98%. Similar findings are obtained in the other investigated scenarios.

In general, we observe a gradual degradation in the performance of these methods as the range increases, especially notable in the Matérn (1.5) and Cauchy models. In all scenarios,

Table 1: Comparison of the relative root mean square error and relative global efficiency of the estimates with respect to the full likelihood, computed from 1000 independent replicates for the exponential model.

		$d_s = 0.05$		$d_s = 0.10$		$d_s = 0.15$	
Range		bi-CL	PCL	bi-CL	PCL	bi-CL	PCL
0.10	σ^2	0.8671	0.7910	0.9515	0.9202	0.9302	0.8568
	ϕ	0.7353	0.2023	0.9051	0.8501	0.8625	0.7419
	τ^2	0.8406	0.7436	0.9340	0.9034	0.8977	0.8183
	Global	0.8386	0.4522	0.9387	0.9103	0.9107	0.8630
0.15	σ^2	0.8827	0.7979	0.9593	0.9231	0.9501	0.8745
	ϕ	0.8006	0.4303	0.8949	0.8524	0.8496	0.7521
	τ^2	0.8484	0.7029	0.9244	0.8865	0.8863	0.7908
	Global	0.8553	0.6206	0.9301	0.9025	0.8986	0.8534
0.20	σ^2	0.8809	0.8062	0.9507	0.9191	0.9423	0.8872
	ϕ	0.8338	0.4718	0.8910	0.8601	0.8466	0.7652
	τ^2	0.8469	0.6751	0.9196	0.8785	0.8763	0.7682
	Global	0.8562	0.6248	0.9227	0.8979	0.8885	0.8406

augmenting d_s to 0.15 adversely affects the estimates of both methods. These results align with existing literature, particularly highlighting the detrimental consequences associated with an excess of terms in the objective function (Bevilacqua and Gaetan, 2015). Notably, when we consider the optimal weighting choice for each method, bi-CL consistently achieves a global efficiency of 85% or higher in all studied scenarios, while this percentage drops to 76% for PCL.

Table 2: Comparison of the relative root mean square error and relative global efficiency of the estimates with respect to the full likelihood, computed from 1000 independent replicates for the Matérn (1.5) model.

		$d_s = 0.05$		$d_s = 0.10$		$d_s = 0.15$	
Range		bi-CL	PCL	bi-CL	PCL	bi-CL	PCL
0.10	σ^2	0.8893	0.8329	0.9461	0.8888	0.9273	0.8348
	ϕ	0.8439	0.7451	0.8851	0.7711	0.8403	0.6441
	τ^2	0.8677	0.7737	0.8879	0.8031	0.8291	0.6919
	Global	0.8624	0.8024	0.9085	0.8398	0.8689	0.7782
0.15	σ^2	0.8668	0.8064	0.9253	0.8866	0.9175	0.8697
	ϕ	0.8025	0.6781	0.8319	0.7428	0.7768	0.6153
	τ^2	0.7716	0.6069	0.8080	0.6850	0.7280	0.5424
	Global	0.8165	0.7219	0.8676	0.7840	0.8162	0.7126
0.20	σ^2	0.8601	0.8148	0.9073	0.8767	0.9023	0.8787
	ϕ	0.7804	0.6432	0.8018	0.7350	0.7448	0.6148
	τ^2	0.7385	0.5371	0.7897	0.6620	0.7020	0.5011
	Global	0.7956	0.6810	0.8514	0.7685	0.7983	0.6906

Table 3: Comparison of the relative root mean square error and relative global efficiency of the estimates with respect to the full likelihood, computed from 1000 independent replicates for the Cauchy model.

		$d_s = 0.05$		$d_s = 0.10$		$d_s = 0.15$	
Range		bi-CL	PCL	bi-CL	PCL	bi-CL	PCL
0.10	σ^2	0.9234	0.9289	0.9485	0.9088	0.9212	0.8303
	ϕ	0.8600	0.7229	0.8879	0.7411	0.8194	0.5579
	τ^2	0.9203	0.9351	0.9274	0.8738	0.8967	0.7850
	Global	0.9017	0.7965	0.9370	0.8743	0.8875	0.7543
0.15	σ^2	0.9037	0.8496	0.9635	0.9220	0.9390	0.8437
	ϕ	0.8716	0.8247	0.8382	0.6904	0.7686	0.5174
	τ^2	0.9110	0.8717	0.8959	0.8142	0.8422	0.6666
	Global	0.8807	0.8428	0.8969	0.8255	0.8457	0.7216
0.20	σ^2	0.8604	0.7785	0.9335	0.8937	0.9202	0.8774
	ϕ	0.8261	0.7660	0.7807	0.6427	0.7056	0.4861
	τ^2	0.8401	0.7464	0.8156	0.7032	0.7411	0.5513
	Global	0.8368	0.7716	0.8515	0.7645	0.7912	0.6713

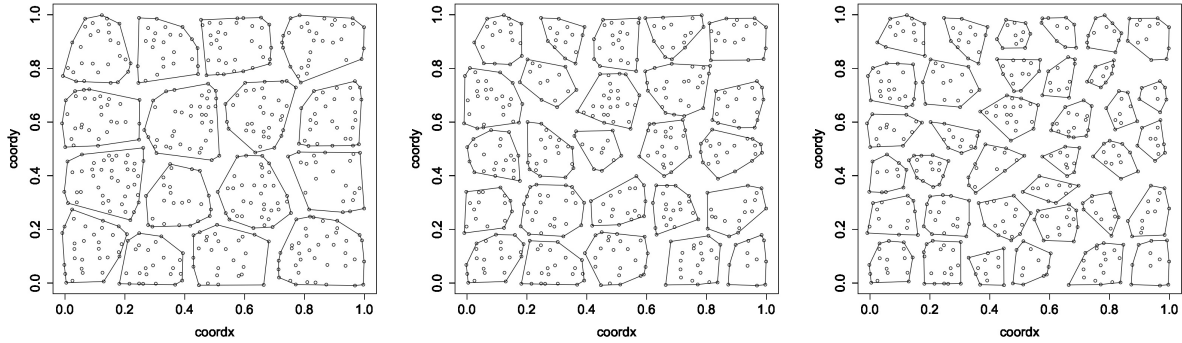


Figure 3: Simulated locations and convex hulls for varying block configurations with 16, 25, and 36 blocks (from left to right).

4.3 Matrix-Free vs. Matrix-Based Methods

We proceed to assess the performance of bi-CL and PCL against the BCL methods described in [Eidsvik et al. \(2014\)](#). Despite all belonging to the same family, they represent opposing extremes within the block likelihood spectrum.

In the same setting as the previous section, with a total of $n = 500$ irregular sites within $[0, 1]^2$, BCL is applied using 16, 25, and 36 blocks. We use the notation BCL_{16} , BCL_{25} , and BCL_{36} for these configurations, respectively. These blocks are constructed through clusters of sites (see [Figure 3](#)). It is worth noting that alternatives such as regular blocking, Voronoi tessellation, or even more intricate structures, are also possible ([Eidsvik et al., 2014](#)), but are not explored here. When forming pairs of blocks to construct the objective function, as detailed in [Section 3.1](#), we specifically consider blocks whose distances, measured between their centers, are less than 0.3, 0.25, and 0.2 for BCL_{16} , BCL_{25} , and BCL_{36} , respectively. These criteria ensure that only neighboring blocks are taken into consideration.

We assess the relative efficiency of BCL methods compared to the full likelihood, examining each parameter individually and employing a global measure, as described in the previous section. This enables us to contrast these efficiencies with those of bi-CL and PCL across the previously described scenarios. To provide a clearer perspective on each

method’s position in this comparison, the results are visually depicted in Figure 4.

The proposed method effectively bridges the gap between PCL and BCL methodologies. Specifically, for the exponential model, matrix-free methods prove notably effective, with bi-CL performing comparably to the best BCL method considered (BCL_{16}). In the Matérn (1.5) model, bi-CL is positioned between BCL_{36} and BCL_{25} . Regarding the Cauchy model, the proposed method demonstrates strong performance when the range is small, comparable to BCL_{16} . However, as the range increases, the method experiences deterioration, mirroring the decline observed in PCL but consistently maintaining superiority over the latter and closely approximating the efficiency of BCL_{25} and BCL_{36} . These results reveal an interesting, and potentially counterintuitive, finding: bi-CL shows efficiencies similar to some matrix-based block likelihood versions.

4.4 Timing Comparison

We proceed to compare the methods in terms of their execution times. These experiments were carried out on a computer with 8GB of memory and a 1.1 GHz Intel Core i3 dual-core processor, ensuring accessibility and replicability for a diverse audience.

In this study, PCL is omitted as its times are found to be quite similar to those of bi-CL. Specifically for BCL, we quantify the time needed for Cholesky factorization, an essential step when dealing with large-sized blocks. We consider two scenarios where the sample is divided into either 8 or 16 blocks of similar size, resembling the cluster-based configurations in Figure 3. The bi-CL method is implemented with $d_s = 0.1$.

In the case of 8 blocks, Cholesky factorization must be applied to matrices of size $n/4 \times n/4$ and computed at least 8 times, especially when the sites are irregularly spaced. This minimum count occurs when each block is paired with its closest counterpart. Therefore, the computed times for the aforementioned matrix operations serve as lower bounds for the BCL evaluations. Similarly, when working with 16 blocks, Cholesky factorization is

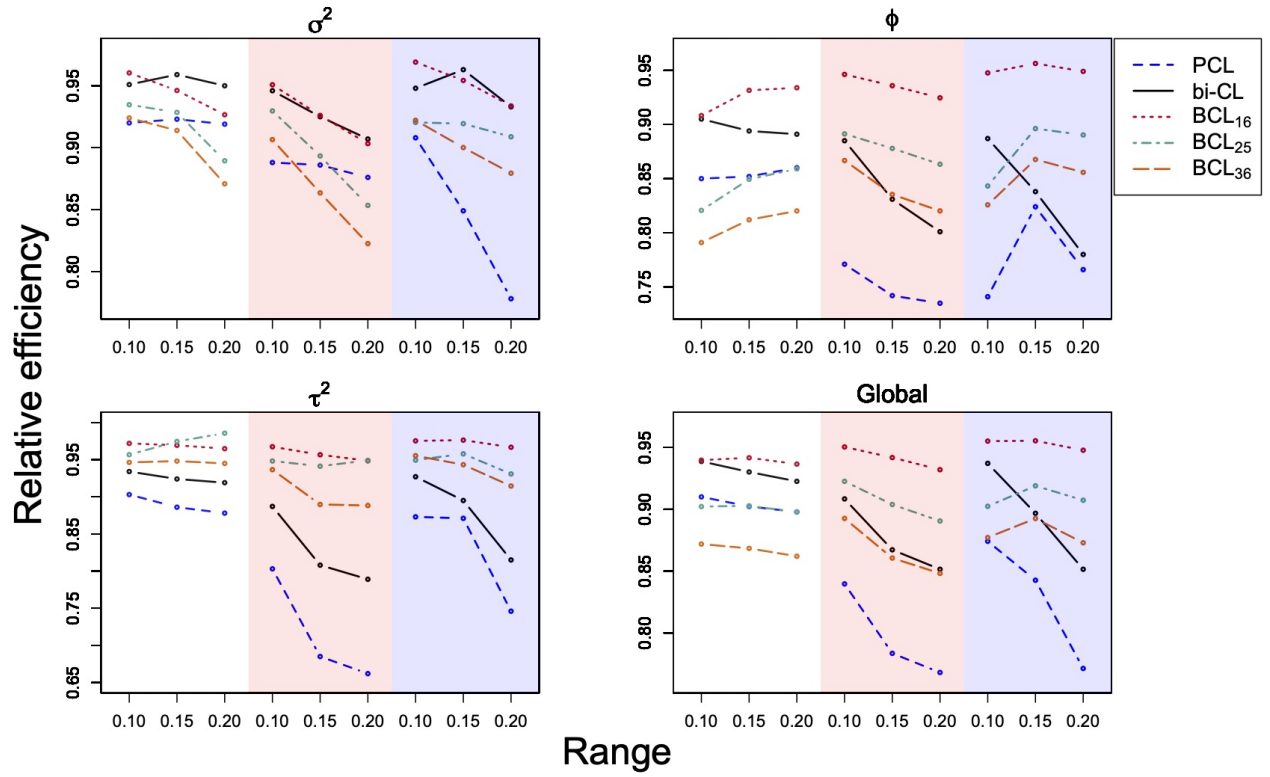


Figure 4: Comparison of the relative root mean square error and relative global efficiency of the estimates with respect to the full likelihood, computed from 1000 independent replicates. The three color zones in each panel correspond to the exponential, Matérn (1.5) and Cauchy models (from left to right). BCL₁₆, BCL₂₅ and BCL₃₆ refer to block likelihood with 16, 25 and 36 blocks, respectively.

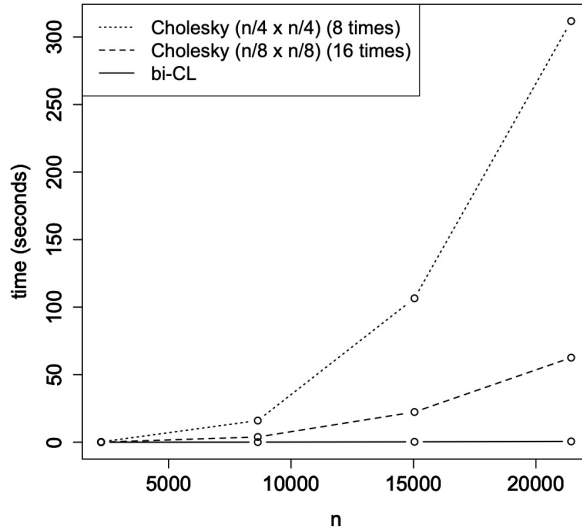


Figure 5: Execution time (in seconds) for evaluating the bi-CL method and the Cholesky factorizations required for BCL_8 and BCL_{16} methods.

required for matrices of size $n/8 \times n/8$ and should be performed at least 16 times.

The results are displayed in Figure 5, considering n ranging from 2,240 to 21,440. This experiment offers insight into the advantage of bi-CL in terms of execution time. The evaluation of the objective function for the method with 16 blocks takes approximately 100 times longer than the evaluation for bi-CL, whereas for the method with 8 blocks, this figure increases to 520 times longer. As these times correspond to a single evaluation, this difference becomes more pronounced proportionally with the number of iterations when maximizing the objective function.

5 Real Data Example

We examine the COBE Sea Surface Temperature data from NOAA PSL in Boulder, Colorado, accessible at <https://psl.noaa.gov> (see Ishii et al., 2005). This dataset, with a spatial resolution of $1^\circ \times 1^\circ$, plays a fundamental role in tracking climate change trends,

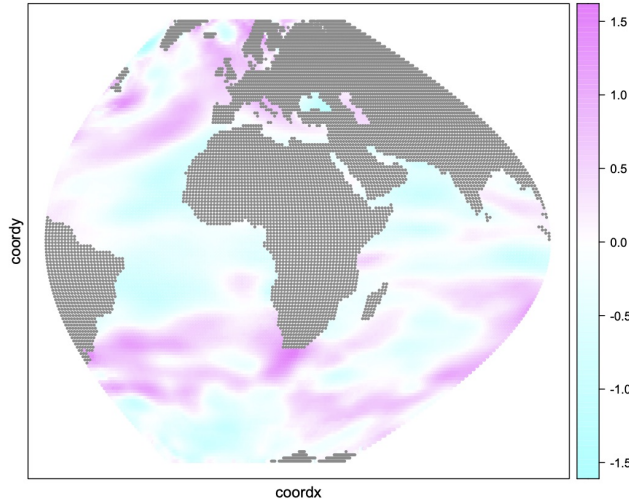


Figure 6: Sea surface temperature anomalies for March 2012, covering a substantial portion of the Earth and measured in degrees Celsius.

gaining insights into ocean circulation patterns, forecasting extreme weather incidents, and influencing policies for marine resource management, as well as reducing the vulnerability of communities to the effects of climate changes.

In our analysis, we focus on the mean anomalies for March 2012 within the study area covering the Atlantic and Indian Oceans. This area corresponds to latitudes between 70°S and 70°N and longitudes between 60°W and 100°E . This enhances the data characterization using an isotropic Gaussian process. Additionally, as a small remnant mean persists, we center the dataset by subtracting the sample mean, which is 0.00968. The resulting dataset comprises 14,884 observations, with locations projected onto the plane using sinusoidal projection (refer to Figure 6).

Given the apparent smoothness in the variable of interest, we employ the Matérn (1.5) covariance function, and the model is augmented with a nugget effect. We estimate the parameters (τ^2, σ^2, ϕ) using both the bi-CL and PCL methods, incorporating a spatial distance threshold for the weights set at $d_s = 500$ km. With a minimum distance of about

39 km between different points in the zone under study, this weighting scheme encompasses a reasonable number of pairs. As in the simulation experiments, the bi-CL method is implemented by adding 5 configurations. Additionally, we implement a large-sized BCL approach with 100 blocks. To ensure computational efficiency, not only for point estimation but also for subsequent standard error calculations, each block is exclusively paired with its nearest neighbor block.

The results are presented in Table 4. Standard errors, enclosed in parentheses within Table 4, are computed using parametric bootstrap, generating 100 replicates based on the estimated models, and subsequently calculating sample standard deviations across these replicates. As discussed in Bai et al. (2012), although this strategy involves more computation, it is less susceptible to bias compared to alternatives based on subsampling techniques. Note that all methods identify an almost negligible nugget effect. While the estimates from all methods are comparable, PCL seems to slightly underestimate the variance and range parameters. Furthermore, PCL exhibits a larger standard error in the estimation of the range compared to its competitors. In contrast, the standard error of the variance estimate is smaller. Figure 7 depicts the sample and fitted semi-variogram for each method, demonstrating a reasonable alignment between theoretical and observed quantities.

We also evaluate the methods concerning predictive performance. Table 4 illustrates the root mean squared error (RMSE) from a leave-one-out prediction study using simple kriging. The methods display similar results, with BCL performing the best, followed by bi-CL, and PCL showing slightly less favorable results. Specifically, the predictive performance gap between PCL and BCL is 7.9%, and bi-CL reduces this gap by approximately 3%. These findings align with the results obtained from experiments using synthetic data, emphasizing the significant role of bi-CL, which positions itself with a level of accuracy between PCL and matrix-based BCL methods.

Table 4: Parameter and standard error estimates for the Matérn (1.5) model with a nugget effect fitted to the sea surface temperature anomalies dataset. The last column also reports the root mean square errors associated to the leave-one-out cross validation study.

	τ^2	σ^2	ϕ	RMSE
bi-CL	0.000916 (0.000075)	0.2207 (0.0308)	2,283 (143.64)	0.02978
BCL	0.000438 (0.000012)	0.2314 (0.0274)	2,381 (101.68)	0.02831
PCL	0.001479 (0.000191)	0.1994 (0.0266)	2,113 (164.19)	0.03077

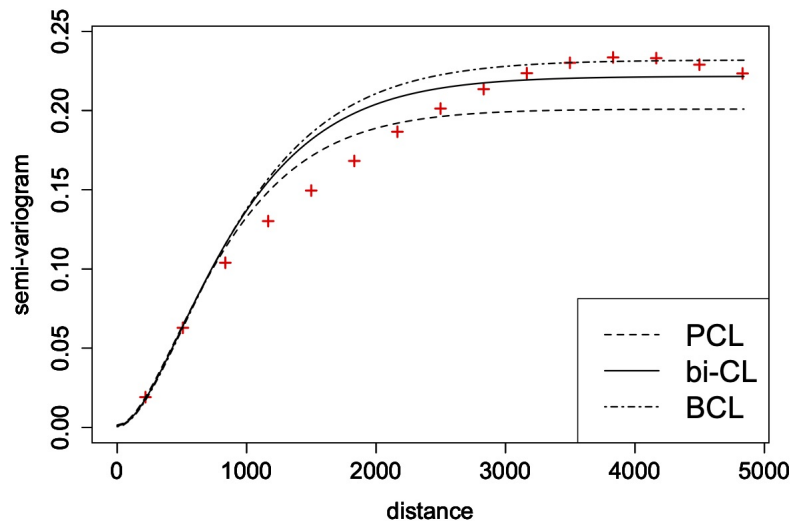


Figure 7: Sample (+) and fitted semi-variograms for sea surface temperature anomalies.

6 Discussion

We introduced the bi-CL method within the spectrum of block likelihoods. Our simulation studies demonstrate the superior performance of this approach compared to the conventional pairwise likelihood method, consistently revealing advantages across diverse scenarios. Significant improvements are observed, particularly for the Matérn (1.5) and Cauchy correlation structures. Importantly, these enhancements come without adding computational complexity.

The proposed methodology also demonstrates comparable efficiencies with matrix-based counterparts, particularly evident in scenarios where the range is small, challenging the intuitive notion that universally increasing block size leads to improved performance.

One strategy to achieve statistical performance closely aligned with the full likelihood involves considering significantly large blocks. However, in this scenario, there is a critical decrease in computational speed. The extent to which one can expand the block size in this method depends on the computational resources available to each user. Apart from this intensive strategy, clear trends correlating block size with statistical improvement are not evident.

Consequently, our proposed approach emerges as a viable alternative. The explicit formulation of our objective function eliminates the need for matrix manipulations. In this way, our study complements the contributions of [Eidsvik et al. \(2014\)](#) by providing additional insights and alternatives to attain a balance between precise statistical estimation and computational efficiency.

Although our primary focus has centered on the estimation problem, we cannot ignore the challenges of kriging prediction in the presence of large datasets, given its dependence on the inverse of the covariance matrix. Therefore, we believe that exploring matrix-free block predictions, as a specific instance of the methodology outlined in [Eidsvik et al. \(2014\)](#), poses a valuable research question deserving further exploration. Given the inherently

local nature of the prediction problem, we anticipate that such a procedure could prove effective. Additional interesting methodologies for exploration in this direction can be found in [Rullièrè et al. \(2018\)](#).

Acknowledgements

The author dedicates this work to his wife, Mariana, and daughter, Celeste, acknowledging their boundless love and constant support.

References

- Aho, A. V. and Hopcroft, J. E. (1974). *The design and analysis of computer algorithms*. Pearson Education India.
- Alegría, A., Caro, S., Bevilacqua, M., Porcu, E., and Clarke, J. (2017). Estimating covariance functions of multivariate skew-Gaussian random fields on the sphere. *Spatial Statistics*, 22:388–402.
- Bai, Y., Song, P. X.-K., and Raghunathan, T. (2012). Joint composite estimating functions in spatiotemporal models. *Journal of the Royal Statistical Society Series B: Statistical Methodology*, 74(5):799–824.
- Banerjee, S., Gelfand, A. E., Finley, A. O., and Sang, H. (2008). Gaussian predictive process models for large spatial data sets. *Journal of the Royal Statistical Society Series B: Statistical Methodology*, 70(4):825–848.
- Bevilacqua, M., Alegria, A., Velandia, D., and Porcu, E. (2016). Composite likelihood inference for multivariate Gaussian random fields. *Journal of Agricultural, Biological, and Environmental Statistics*, 21:448–469.

- Bevilacqua, M. and Gaetan, C. (2015). Comparing composite likelihood methods based on pairs for spatial Gaussian random fields. *Statistics and Computing*, 25:877–892.
- Bevilacqua, M., Gaetan, C., Mateu, J., and Porcu, E. (2012). Estimating space and space-time covariance functions for large data sets: a weighted composite likelihood approach. *Journal of the American Statistical Association*, 107(497):268–280.
- Caamaño-Carrillo, C., Bevilacqua, M., López, C., and Morales-Oñate, V. (2024). Nearest neighbors weighted composite likelihood based on pairs for (non-) Gaussian massive spatial data with an application to Tukey-hh random fields estimation. *Computational Statistics & Data Analysis*, 191:107887.
- Cao, J., Genton, M. G., Keyes, D. E., and Turkiyyah, G. M. (2021). Sum of Kronecker products representation and its Cholesky factorization for spatial covariance matrices from large grids. *Computational Statistics & Data Analysis*, 157:107165.
- Caragea, P. C. and Smith, R. L. (2007). Asymptotic properties of computationally efficient alternative estimators for a class of multivariate normal models. *Journal of Multivariate Analysis*, 98(7):1417–1440.
- Castruccio, S., Huser, R., and Genton, M. G. (2016). High-order composite likelihood inference for max-stable distributions and processes. *Journal of Computational and Graphical Statistics*, 25(4):1212–1229.
- Chiles, J.-P. and Delfiner, P. (2012). *Geostatistics: modeling spatial uncertainty*, volume 713. John Wiley & Sons.
- Cressie, N. (2015). *Statistics for spatial data*. John Wiley & Sons.
- Curriero, F. C. and Lele, S. (1999). A composite likelihood approach to semivariogram estimation. *Journal of Agricultural, Biological, and Environmental Statistics*, 4(1):9–28.

- Eidsvik, J., Shaby, B. A., Reich, B. J., Wheeler, M., and Niemi, J. (2014). Estimation and prediction in spatial models with block composite likelihoods. *Journal of Computational and Graphical Statistics*, 23(2):295–315.
- Fuentes, M. (2007). Approximate likelihood for large irregularly spaced spatial data. *Journal of the American Statistical Association*, 102(477):321.
- Furrer, R., Genton, M. G., and Nychka, D. (2006). Covariance tapering for interpolation of large spatial datasets. *Journal of Computational and Graphical Statistics*, 15(3):502–523.
- Heagerty, P. J. and Lele, S. R. (1998). A composite likelihood approach to binary spatial data. *Journal of the American Statistical Association*, 93(443):1099–1111.
- Heaton, M. J., Datta, A., Finley, A. O., Furrer, R., Guinness, J., Guhaniyogi, R., Gerber, F., Gramacy, R. B., Hammerling, D., Katzfuss, M., et al. (2019). A case study competition among methods for analyzing large spatial data. *Journal of Agricultural, Biological and Environmental Statistics*, 24:398–425.
- Hong, Y., Song, Y., Abdulah, S., Sun, Y., Ltaief, H., Keyes, D. E., and Genton, M. G. (2023). The third competition on spatial statistics for large datasets. *Journal of Agricultural, Biological and Environmental Statistics*, 28:618–635.
- Huang, H., Abdulah, S., Sun, Y., Ltaief, H., Keyes, D. E., and Genton, M. G. (2021). Competition on spatial statistics for large datasets. *Journal of Agricultural, Biological and Environmental Statistics*, 26:580–595.
- Ishii, M., Shouji, A., Sugimoto, S., and Matsumoto, T. (2005). Objective analyses of sea-surface temperature and marine meteorological variables for the 20th century using icoads and the kobe collection. *International Journal of Climatology*, 25(7):865–879.
- Katzfuss, M. and Guinness, J. (2021). A General Framework for Vecchia Approximations of Gaussian Processes. *Statistical Science*, 36(1):124 – 141.

- Kaufman, C. G., Schervish, M. J., and Nychka, D. W. (2008). Covariance tapering for likelihood-based estimation in large spatial data sets. *Journal of the American Statistical Association*, 103(484):1545–1555.
- Lindgren, F., Rue, H., and Lindström, J. (2011). An explicit link between Gaussian fields and Gaussian Markov random fields: the stochastic partial differential equation approach. *Journal of the Royal Statistical Society Series B: Statistical Methodology*, 73(4):423–498.
- Lindsay, B. G. (1988). Composite likelihood methods. *Comtemporary Mathematics*, 80(1):221–239.
- Litvinenko, A., Kriemann, R., Genton, M. G., Sun, Y., and Keyes, D. E. (2020). Hlibcov: Parallel hierarchical matrix approximation of large covariance matrices and likelihoods with applications in parameter identification. *MethodsX*, 7:100600.
- Ruli, E., Sartori, N., and Ventura, L. (2016). Approximate Bayesian computation with composite score functions. *Statistics and Computing*, 26(3):679–692.
- Rullière, D., Durrande, N., Bachoc, F., and Chevalier, C. (2018). Nested kriging predictions for datasets with a large number of observations. *Statistics and Computing*, 28:849–867.
- Sang, H. and Genton, M. G. (2014). Tapered composite likelihood for spatial max-stable models. *Spatial Statistics*, 8:86–103.
- Shaby, B. and Ruppert, D. (2012). Tapered covariance: Bayesian estimation and asymptotics. *Journal of Computational and Graphical Statistics*, 21(2):433–452.
- Stein, M. L. (2012). *Interpolation of spatial data: some theory for kriging*. Springer Science & Business Media.
- Stein, M. L., Chen, J., and Anitescu, M. (2013). Stochastic approximation of score functions for Gaussian processes. *The Annals of Applied Statistics*, 7(2):1162 – 1191.

- Stein, M. L., Chi, Z., and Welty, L. J. (2004). Approximating likelihoods for large spatial data sets. *Journal of the Royal Statistical Society Series B: Statistical Methodology*, 66(2):275–296.
- Sun, Y. and Stein, M. L. (2016). Statistically and computationally efficient estimating equations for large spatial datasets. *Journal of Computational and Graphical Statistics*, 25(1):187–208.
- Varin, C. (2008). On composite marginal likelihoods. *AStA Advances in Statistical Analysis*, 92(1):1–28.
- Varin, C., Reid, N., and Firth, D. (2011). An overview of composite likelihood methods. *Statistica Sinica*, 21(1):5–42.
- Vecchia, A. V. (1988). Estimation and model identification for continuous spatial processes. *Journal of the Royal Statistical Society Series B: Statistical Methodology*, 50(2):297–312.
- Whittle, P. (1954). On stationary processes in the plane. *Biometrika*, 41(3/4):434–449.